A Global Analysis of Pre-seismic Related Ionospheric Anomalies

Luke Cullen [1,2], Asadullah H Galib [1,3], Andy W Smith [1,3,4], Debvrat Varshney [1,6], Edward Brown [1,2], Peter J Chi [1,6], Xiangning Chu [1,6], Filip Svoboda [1,2]

[1]Frontier Development Lab, Sunnyvale, CA, USA
[2]Department of Engineering, University of Cambridge, UK
[3]Michigan State University, USA
[4]Northumbria University, UK
[5]University College London, UK
[6]University of Maryland Baltimore County, USA
[7]University of California Los Angeles, USA

Key Points:

- enter point 1 here
- enter point 2 here
- enter point 3 here

Corresponding author: =name=, `=email address=`

Abstract

The ionosphere is the upper, ionized layer of Earth's atmosphere. During seismic events, such as earthquakes, the ionosphere is perturbed. In this work, we use over 20 years of data from earthquakes around the world, with measurements of ionospheric density to show that the impact of these perturbations can be observed in even low time and spatial resolution ionospheric density data, with statistically significant ($p \leq 0.01$) deviations from the previous day.

Dependence upon earthquake parameters and regional properties

Pre-earthquake

Plain Language Summary

[enter your Plain Language Summary here or delete this section]

1 Introduction

The ionosphere is one of the upper layers of Earth's atmosphere, located at altitudes greater than $\sim$ 50 km . It is ionized through its illumination with solar UV radiation and the precipitation of energetic particles from near-Earth space (). The ionosphere varies with many factors including: the time of day, latitude, and the levels of solar and geomagnetic activity (). These changes can impact the propagation of radio signals, interfere with communication systems and degrade the accuracy of navigation tools ().

However, we can remotely monitor the ionosphere through the impact of its content on GNSS (Global Navigation Satellite Systems) signals. Dual-frequency GNSS receivers can be used to calculate the integrated electron density (total electron content: TEC) along the line of sight to the spacecraft. This can be later converted into the vTEC, or vertical total electron content.

While most factors that impact the ionosphere are external in origin (e.g. solar illumination), it can also be impacted by geological and seismic events. For example, during the 2011 Tohoku earthquake (Rolland et al., 2011) and the recent Tonga eruption (Zhang et al., 2022).

Post-earthquake gravity waves.

Galvan et al. (2011) showed that two earthquakes in 2009 and 2010 (in Samoa and Chile) were associated with fluctuations in TEC. However they also showed that the tsunami related events only had a typical amplitude of $\sim 0.1 - 0.2$TECU.

Recently, Astafyeva and Shults (2019) demonstrated the impact down to magnitude 7.4.

(Sithartha Muthu Vijayan & Shimna, 2022) assessed the impact of non-uniform sampling and aliasing on the detection of seismogenic ionospheric perturbations, finding that they must be considered to distinguish these perturbations from the background, increasing the signal to noise ratio significantly.

It has also been suggested that there are changes in the ionosphere in the days () or weeks () prior to an earthquake occurring.

Decrease in TEC 3 - 5 days before earthquakes in China (M > 6.3) (J. Y. Liu et al., 2009), while later work (M > 6) suggested that pre-earthquake TEC anomalies depend on local time, and that TEC can be enhanced or decreased (C. Y. Liu et al., 2018). May be a statistical artifact (Ikuta & Oba, 2022).

Thomas et al. (2017) completed a global study, concluding that there was no consistent, global signature in the days before an earthquake. However, Thomas et al. (2017) note that it is possible that these are localized and last a few hours. Zhu and Jiang (2020) looked at ionospheric distrurbances up to 15 days before earthquakes, limiting their sample to those inland due to GPS data coverage, once more concluding that there were little to no consistent signatures.

(Ulukavak et al., 2020) positive and negative TEC anomalies in the 15 days before an earthquake.

Issues with accounting for data quality, "anomaly" definitions and such are problematic, though the field shows some promise (Lim & Leong, 2019).

In this work, we statistically assess whether the ionospheric perturbations from seismic events can be identified, by comparing the changes within a region over a day. We make as few downselections as possible. Nonetheless we show that a lightweight monitor, comparing statistical parameters within regions of the ionosphere, may be suitable to identify the ionospheric precursor of earthquakes.

2 Data

Here we use data from the Madrigal database [cedar.openmadrigal.org] which provides global maps of vertical TEC, calculated from GNSS data (Rideout & Coster, 2006). This data are provided on a 1° by 1° grid at a temporal cadence of 5 minutes. We note here that though global, the data are incomplete, with typical global completeness of $\sim$ 25% (e.g. Sun et al., 2022).

We use the USGS earthquake catalog to identify and classify earthquakes (USGS, 2022). This catalog records critical features such as the timing, magnitude (M), location and depth of earthquakes.

To maximize data completeness while permitting the largest possible set of historical data, we use the period between 2000 and 2020 as our statistical sample.

Regions

3 Method

Ionospheric TEC is influenced by a large number of contributing factors. These factors include solar illumination and incident energetic particle flux, meaning that TEC will vary annually, diurnally and stochastically depending on the current space weather conditions. To enable us to probe the impact of seismic effects we choose to compare the observed TEC value to those obtained 24 hours before. We do not remove events during geomagnetically active intervals (c.f. Thomas et al., 2017).

Due to data availability (discussed above) it is not always possible to compare the TEC value at a specific location, nor would we wish to do so. For this reason we instead evaluate the statistical properties (e.g. mean/median) of a region of the ionosphere, e.g. $\pm X^\circ$ of longitude and latitude. In particular, we compare the median observed TEC to those obtained the day before using the following equations:

$$\text{TEC}_{\text{Anomaly}} = < \text{TEC} >_{T0} - < \text{TEC} >_{T0-24h} \tag{1}$$

where the $< \text{TEC} >$ is the median of the TEC values measured within a defined region, requiring that there are at least two data points recorded. We ignore any epochs for which this cannot be calculated due to a lack of data.

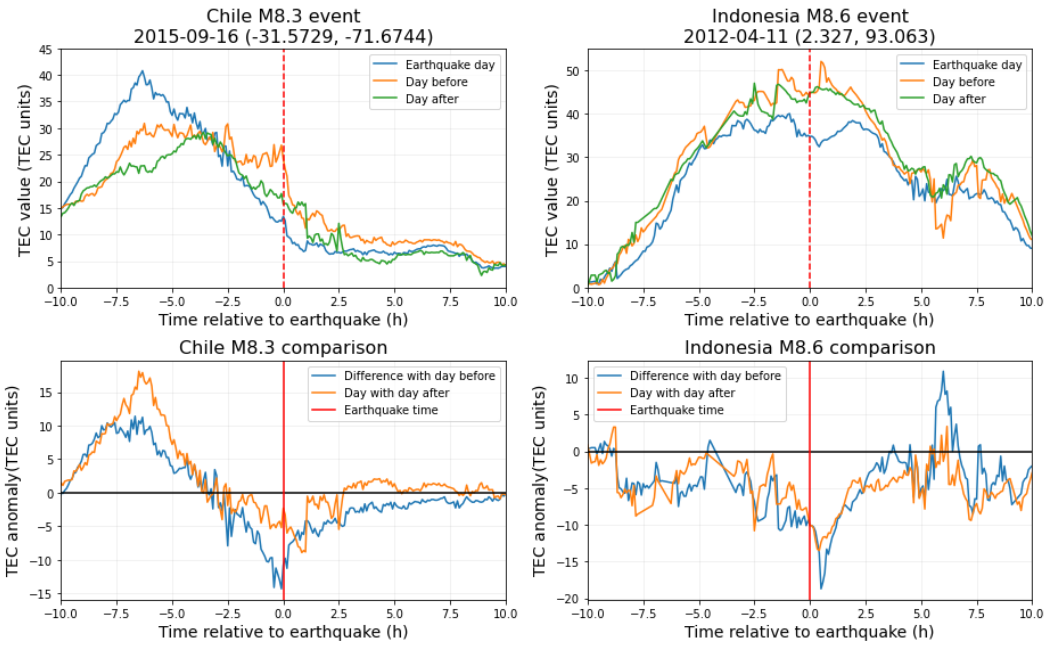

Figure 1. Case study

Wilcoxon test - how we determine significance.

4 Results

4.1 Example

Figure **??** details a superposed epoch analysis of the change in ionospheric TEC measured $\pm 3^\circ$ of the earthquake epicenter, for earthquakes greater than magnitude 7. Figure **??**a shows the difference in the spatial range of TEC, with the median and interquartile range of the distribution marked. Figure **??**b then shows the p-value (significance) of the distribution of TEC differences at each epoch, evaluated with the Wilcoxon test. Here we take anything with a p-value less than 0.2 to be significant for our purposes.

From Figure **??** we can see that before the earthquakes zero change in TEC is well within the interquartile range, and the median change is TEC is often around ~ 0. In contrast, in the hour following an earthquake the median change in range of TEC from the day before is mostly greater than zero, $\sim 2 TECunits$. The interquartile range is almost entirely above zero for this hour.

The significance of this shift is confirmed in Figure **??**b, where the p values returned by the Wilcoxon test are entirely below 0.2, and reach as low a 0.002 around 30 minutes after the earthquake.

4.2 Dependence on Magnitude and Region Definition

Above, Figure **??** shows the statistics for a specific region around earthquakes ($\pm 3^\circ$) and for earthquakes larger than a given magnitude (greater than magnitude 7). We now examine how the results displayed depend upon these choices. Figure 1 shows three panels examining these relationships. Figure 1b shows the p value of the most significant epoch in the hour following the earthquakes - calculated via the Wilcoxon test - com-

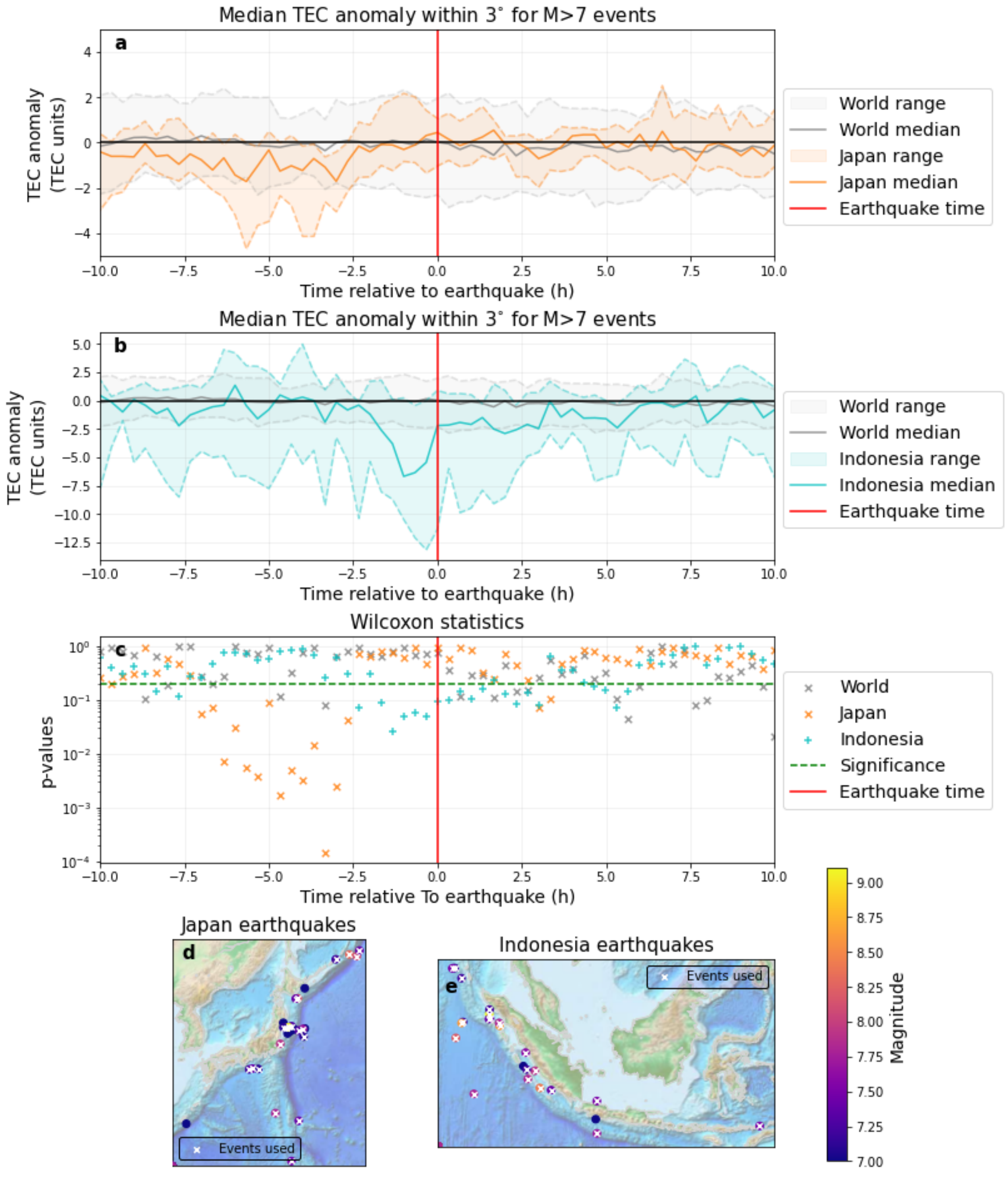

Figure 2. Japan and Indonesia drops in TEC

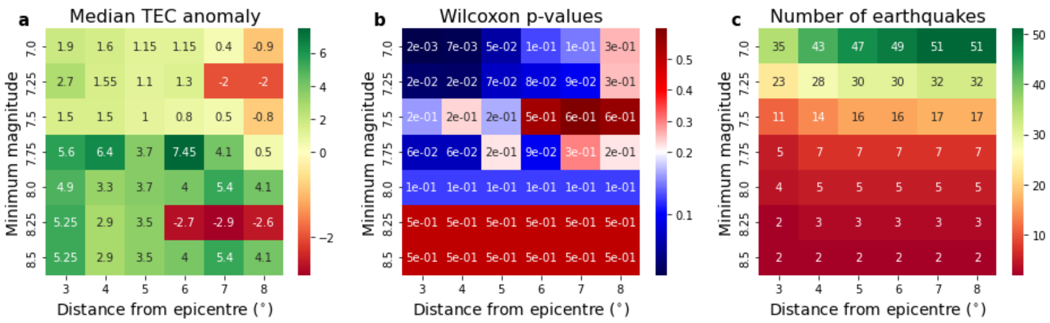

Figure 3. Heatmaps of dependance on region and magnitude observed

paring the distribution of TEC anomalies, as a function of minimum magnitude and regional extent (in degrees). Here, we have chosen a significance level of 0.2, values larger than this are colored red, while more significant values are blue. Figure 1a then shows the median TEC anomaly (for the most significant epoch) with green colors indicating a larger anomaly and red indicating reduced variability. We note that the most significant epoch may not correspond to the largest median TEC anomaly as the significance of the distribution is tested, and not the significance of the median value. Figure 1c then shows the support behind the statistics: the number of earthquakes in the sample from which they are calculated.

We can see that for earthquakes greater than magnitude 7 we see a significant increase in the observed range of TEC. The median TEC anomaly is approximately 2 TECU within 3° and reduces as the region considered increases. As the magnitude increases we see that the median TEC anomaly increases (e.g. moving down Figure 1a), though the significance decreases - likely as the number of earthquakes in the sample decreases (Figure 1c). Broadly this is the case for all combinations tested, we see that placing a larger limit on the magnitude increase the TEC anomaly observed, but the statistical significance decreases with the smaller sample size.

4.3 Regional Dependence

We next examine how the observations apply to two key regions: the Indonesian and Japanese subduction zones.

5 Discussion

5.1 Data Scarcity

5.2 Data Resolution

Thomas et al. (2017), (Zhu & Jiang, 2020) and (Ulukavak et al., 2020) found little to no clear signatures, but removed diurnal trends and geomagnetically active days. Low resolution (2.5 latitude, 5 degree longitude and 2 hour cadence).

6 Conclusion

7 Open Research

Acknowledgments

This work has been enabled by the Frontier Development Lab Program (FDL). FDL is a collaboration between SETI Institute and Trillium Technologies Inc., in partnership with Department of Energy (DOE), National Aeronautics and Space Administration (NASA), and U.S. Geological Survey (USGS), SETI Institute, and Trillium Technologies Inc., in partnership with private industry and academia. This public/private partnership ensures that the latest tools and techniques in Artificial Intelligence (AI) and Machine Learning (ML) are applied to basic research priorities in support of science and exploration of material concerns to human kind. The material is based upon work supported by NASA under award No(s) NNX14AT27A.

References

Astafyeva, E., & Shults, K. (2019). Ionospheric gnss imagery of seismic source: Possibilities, difficulties, and challenges. *Journal of Geophysical Research: Space Physics*, *124*(1), 534-543. Retrieved from `https://agupubs.onlinelibrary.wiley.com/doi/abs/10.1029/2018JA026107` doi: https://doi.org/10.1029/2018JA026107

Galvan, D. A., Komjathy, A., Hickey, M. P., & Mannucci, A. J. (2011). The 2009 samoa and 2010 chile tsunamis as observed in the ionosphere using gps total electron content. *Journal of Geophysical Research: Space Physics*, *116*(A6). Retrieved from `https://agupubs.onlinelibrary.wiley.com/doi/abs/10.1029/2010JA016204` doi: https://doi.org/10.1029/2010JA016204

Ikuta, R., & Oba, R. (2022). How credible are earthquake predictions based on tec variations? *Journal of Geophysical Research: Space Physics*, *127*(3), e2021JA030151. Retrieved from `https://agupubs.onlinelibrary.wiley.com/doi/abs/10.1029/2021JA030151` (e2021JA030151 2021JA030151) doi: https://doi.org/10.1029/2021JA030151

Lim, B. J., & Leong, E. C. (2019, jun). Challenges in the Detection of Ionospheric Pre-Earthquake Total Electron Content Anomalies (PETA) for Earthquake Forewarning. *Pure and Applied Geophysics*, *176*(6), 2425–2449. Retrieved from `https://link.springer.com/article/10.1007/s00024-018-2083-7` doi: 10.1007/S00024-018-2083-7/FIGURES/17

Liu, C. Y., Liu, J. Y., Chen, Y. I., Qin, F., Chen, W. S., Xia, Y. Q., & Bai, Z. Q. (2018, oct). Statistical analyses on the ionospheric total electron content related to M 6.0 earthquakes in China during 1998 - 2015. *Terrestrial, Atmospheric and Oceanic Sciences*, *29*(5), 485–498. Retrieved from `http://tao.cgu.org.tw/index.php/articles/archive/geophysics/item/1595` doi: 10.3319/TAO.2018.03.11.01

Liu, J. Y., Chen, Y. I., Chen, C. H., Liu, C. Y., Chen, C. Y., Nishihashi, M., ... Lin, C. H. (2009). Seismoionospheric gps total electron content anomalies observed before the 12 may 2008 mw7.9 wenchuan earthquake. *Journal of Geophysical Research: Space Physics*, *114*(A4). Retrieved from `https://agupubs.onlinelibrary.wiley.com/doi/abs/10.1029/2008JA013698` doi: https://doi.org/10.1029/2008JA013698

Rideout, W., & Coster, A. (2006, jul). Automated GPS processing for global total electron content data. *GPS Solutions*, *10*(3), 219–228. Retrieved from `https://link.springer.com/article/10.1007/s10291-006-0029-5` doi: 10.1007/S10291-006-0029-5/FIGURES/6

Rolland, L. M., Lognonné, P., Astafyeva, E., Kherani, E. A., Kobayashi, N., Mann, M., & Munekane, H. (2011, sep). The resonant response of the ionosphere imaged after the 2011 off the Pacific coast of Tohoku Earthquake. *Earth, Planets and Space*, *63*(7), 853–857. Retrieved from https://link.springer.com/articles/10.5047/eps.2011.06.020https://link.springer.com/article/10.5047/eps.2011.06.020 doi: 10.5047/EPS.2011.06.020/FIGURES/4

Sithartha Muthu Vijayan, M., & Shimna, K. (2022). Detecting aliasing and artifact free co-seismic and tsunamigenic ionospheric perturbations using gps. *Advances in Space Research*, *69*(2), 951-975. Retrieved from https://www.sciencedirect.com/science/article/pii/S0273117721008000 doi: https://doi.org/10.1016/j.asr.2021.10.040

Sun, H., Hua, Z., Ren, J., Zou, S., Sun, Y., & Chen, Y. (2022). Matrix completion methods for the total electron content video reconstruction. *The Annals of Applied Statistics*, *16*(3), 1333–1358.

Thomas, J. N., Huard, J., & Masci, F. (2017). A statistical study of global ionospheric map total electron content changes prior to occurrences of m6.0 earthquakes during 2000–2014. *Journal of Geophysical Research: Space Physics*, *122*(2), 2151-2161. Retrieved from https://agupubs.onlinelibrary.wiley.com/doi/abs/10.1002/2016JA023652 doi: https://doi.org/10.1002/2016JA023652

Ulukavak, M., Yalçınkaya, M., Kayıkçı, E. T., Öztürk, S., Kandemir, R., & Karslı, H. (2020, apr). Analysis of ionospheric TEC anomalies for global earthquakes during 2000-2019 with respect to earthquake magnitude (Mw6.0). *Journal of Geodynamics*, *135*, 101721. doi: 10.1016/J.JOG.2020.101721

USGS. (2022). Search earthquake catalog. *Earthquake Hazards Program*. Retrieved from https://earthquake.usgs.gov/earthquakes/search/

Zhang, S. R., Vierinen, J., Aa, E., Goncharenko, L. P., Erickson, P. J., Rideout, W., ... Spicher, A. (2022, mar). 2022 Tonga Volcanic Eruption Induced Global Propagation of Ionospheric Disturbances via Lamb Waves. *Frontiers in Astronomy and Space Sciences*, *9*, 49. doi: 10.3389/FSPAS.2022.871275/BIBTEX

Zhu, F., & Jiang, Y. (2020, oct). Investigation of GIM-TEC disturbances before M6.0 inland earthquakes during 2003–2017. *Scientific Reports 2020 10:1*, *10*(1), 1–7. Retrieved from https://www.nature.com/articles/s41598-020-74995-w doi: 10.1038/s41598-020-74995-w